



## Performance analysis of microbial fuel cell operational parameters on reactive azo dye decolorization

R. Ilamathi, A. Merline Sheela\*

Centre for Environmental Studies, College of Engineering, Anna University, Chennai-600 025, India, emails: merline@annauniv.edu (A.M. Sheela), mathidmagnate@gmail.com (R. Ilamathi)

Received 12 September 2019; Accepted 6 February 2020

---

### ABSTRACT

Microbial fuel cell design was used to identify the effect of different catholyte and anolyte to improve the performance of reactive azo dye (Reactive Orange 16) treatment using *Pseudomonas aeruginosa* as biocatalyst. Supplementation with potassium permanganate, potassium ferricyanide, manganese dioxide, potassium chromate, and aromatic amines reduced dye degradation efficiency. Higher open circuit potential ( $1.15 \pm 0.05$  V) was obtained using potassium permanganate as a cathodic electron acceptor with the dye decolorization efficiency of  $69\% \pm 1.2\%$ . Glucose, sucrose, acetate, glycerol, and mannitol were examined separately for decolorization with simultaneous bioelectricity generation. Increased decolorization was achieved with glucose followed by sucrose, acetate, glycerol, and mannitol. Glucose yielded the maximum power density of  $1.9 \pm 0.18$  mW m<sup>-2</sup> for  $97\% \pm 0.8\%$  decolorization. UV-visible spectra, Fourier-transform infrared spectroscopy, and gas-chromatography–mass spectrometry–gas-chromatograph–mass spectrometer analysis confirmed the presence of degraded metabolites.

*Keywords:* Dye degradation; Reactive azo dye; Microbial fuel cell; GC/MS; Azoreductase

---

### 1. Introduction

Azo dye account for the majority of textile dyestuffs and they are the commonly used synthetic dyes in various industries like textile, paper, food, cosmetics, pharmaceutical industries, etc. [1]. Among the dyes used, pollution associated with reactive dyes account for a notable proportion in the overall dye market. Residual color is a major problem with reactive azo dyes, because, during the dyeing processes, up to 50% of the reactive dye that present in the original dye bath is lost to the wastewater due to the low levels of dye-fibre fixation [2,3]. Due to their stability and xenobiotic nature, reactive azo dyes were not degraded completely by conventional wastewater treatment. Various physico-chemical treatment of dye degradation have certain problems such as production of more sludge and are inefficient, costly and are of limited application. Biological degradation for the

treatment of textile dye has received more attention now-a-days as the green approach. Therefore, the dyeing industries are compelled to search for innovative novel treatments that are directed particularly towards the decolorization of textile effluent. In this scenario, microbial fuel cell (MFC) represents a novel and upcoming method for the treatment of dye effluent, considering as an environmentally friendly and cost-effective alternative to other physico-chemical treatment.

MFC converts the chemical energy from the fuel to electrical energy by the catalytic action of microorganisms. It consists of two compartments: Anode and cathode separated by a proton exchange membrane (PEM) [4]. Utilization of microbial fuel system for practical applications of energy production transforming the textile wastewater disposal into electricity are being extensively studied in recent years [5]. MFCs have been demonstrated as a promising

---

\* Corresponding author.

and challenging technology in addressing dye wastewater treatment with energy recovery. Although the present applications of MFCs are still at lab-scale, but have been proved to be of potential industrial applications. Electricity generation from acetate, glucose, and ethanol using MFC application are well known [6–8]. But very few work devoted to electricity generation from these substrates during dye degradation. MFC can utilize various substrates ranging from carbohydrates to wastewater compounds in anolyte using anode as the electron acceptor [7]. Major drawback of this system is that bacterial strains cannot use dye as a growth substrate because of complex structure of the dye molecule and the conditions. Thus, it undergoes the reductive cleavage and the dye decolorization may compete with the electron transfer at the anode in MFCs. Hence to improve the MFC performance as well as the ability to degrade the azo dyes, a serious threat in treating prevails due to its complex and toxic nature in addition with the need for electron shuttle capability [9].

In MFCs, the performance of the cathode has been considered to be the major limiting factor in MFC power generation [10]. In conventional MFCs, cathodes are placed in the catholyte solution where they are sparged with air to provide oxygen for the electrode. Using oxidizing agents in the catholyte the power density, as well as azo dye decolorization efficiency, increased [8]. Major advantage of catholyte in MFCs is of greater mass transfer which relatively increases solution's redox potential than dissolved oxygen. Thereby, it fasters the reduction kinetics more compared to that of oxygen [11]. The widely used and effective catholytes for azo dye treatment are potassium permanganate, potassium ferricyanide, and phosphate buffer [12,13]. The anolyte determines the power output of MFC and the dye wastewater with inoculated biomass is the most common anolytic solution in MFC for textile effluent treatment [14]. Addition of extraneous mediators in anolyte depends on the type of microbial inoculums employed in MFC system to attain higher power density [4].

The main objective of this study is to explore the effective catholytes and the possibility of employing various anolyte for the fastest decolorization of azo dye. The integration of MFC, dye wastewater treatment with oxidative/reductive enzyme for textile effluent treatment was reported for the cost-effective treatment process. Further, MFCs decolorization conditions and electricity production by *Pseudomonas aeruginosa* were studied in detail using the two model dye RO-16 and RB-5. Furthermore, the transfer of intermediate products of RO-16 and RB-5 were explored using MFC system.

## 2. Materials and methods

### 2.1. MFC reactor configuration

A bottle type H-shaped MFC (14 cm × 7 cm) with a working volume of about 0.15 L was used with the cathode and anode chambers separated by a PEM (Nafion 117, Dupont Co., Fayetteville, NC). Graphite electrodes were placed and were connected across a resistor of 220 Ω. Graphite block (14.8 cm<sup>2</sup>) was soaked in ethanol for 3 h and then washed in deionized water and dried for 1 h before starting MFC operation. Ag/AgCl reference electrode (+0.2 V vs. normal hydrogen electrode) was used to measure the electrode potentials.

Pigment producing *P. aeruginosa* microbial type culture collection 2582 was obtained from Institute of Microbial Technology, Chandigarh was fed into the anodic chamber. The reactor was run for a period of 360 h with synthetic feed solution mineral salt medium (MSM): KH<sub>2</sub>PO<sub>4</sub>, 13.6 g/L; Na<sub>2</sub>SO<sub>4</sub>, 9.47 g/L; NaOH, 2.33 g/L; NH<sub>4</sub>Cl, 0.45 g; MgSO<sub>4</sub>·7H<sub>2</sub>O, 0.17 g/L; FeCl<sub>3</sub>, 1.00 mg/L; MnCl<sub>2</sub>·4H<sub>2</sub>O 23.0 mg/L; CaCl<sub>2</sub>·2H<sub>2</sub>O 15.0 mg/L; Glucose 10 g/L, final pH 7.0 ± 0.2 (Hi Media Laboratories Pvt., Ltd., India) at 37°C [15]. The species was slowly acclimated in minimal salt media ranging from 10% to 100% with dye and without dye for fuel cell experiments. Both the acclimated and unacclimated cultures were stored at 5°C in the refrigerator and subcultured every month in MSM agar with glucose (10 g/L). Microorganism was maintained on Modified King's B medium (3 g K<sub>2</sub>HPO<sub>4</sub>, 13.3 g Glucose, 0.65 g Na<sub>2</sub>HPO<sub>4</sub>, 1 g MgSO<sub>4</sub>, and 1 g NH<sub>4</sub>Cl per liter, pH 7.0). About 5 mL of the culture (0.25 ± 0.02 g dry cell weight/L) was used as inoculum for each MFC set-up.

### 2.2. Effect of catholyte and anolyte

The anode chamber was kept anaerobic during the operation time with Reactive Orange 16 (RO-16) as model dye solution tested for azo dye decolorization. The anode was purged with nitrogen for 20 mins at an interval of 24 h to maintain the anaerobic condition in the anode chamber. The MFC was operated in batch condition at room temperature over a period of 360 h. Potassium permanganate, potassium ferricyanide, potassium dichromate, manganese dioxide, potassium chromate, aromatic amines in 50 mM of phosphate buffer concentration was tested at pH 7.0 to determine the suitable and efficient catholyte for azo dye decolorization in MFC. The catholyte for each MFC was prepared at 25 mM operated in open circuit mode, to reach maximum voltage using 220 Ω to determine the chemical oxygen demand (COD) reduction [16]. In a few experiments, air pump was used to supply oxygen in each set-up. The membranes were pre-treated with 1% H<sub>2</sub>O<sub>2</sub> (v/v) and 0.5 M H<sub>2</sub>SO<sub>4</sub> solution for 1 h and then soaked with deionized water. Similarly, co-substrate (10 g/L) was added in anolyte before every start-up of MFC and the phosphate buffer saline (PBS) (50 mM; pH7.0) was fed into the cathode chamber in batch mode. Glucose, sucrose, glycerol, acetate, and mannitol was charged for every cycle in the anode solution and the efficiency of azo dye decolorization, voltage generation, and COD removal was recorded for each MFC run.

### 2.3. Enzymatic analysis

Azoreductase enzyme assays were carried out in reaction mixture 2.0 mL containing 0.1 M of methyl red in phosphate buffer (50 mM; pH 7.5) and 0.2 mL of enzyme solution. Reaction was initiated by adding 100 μM of NADH and the decrease in optical density (OD) at 430 nm was observed. The molar extinction co-efficient of azo dye (methyl red) was 0.023 μM<sup>-1</sup> cm<sup>-1</sup> reported in [17]. Laccase activity was determined in a reaction mixture (2.0 mL of 10% 2,2'-azino-bis(3-ethylbenzothiazoline-6-sulfonic acid (ABTS)) containing 1.7 mL acetate buffer (20 mM, pH 4.0) and measured the increase in OD at 420 nm [18]. The amount of enzyme required to reduce 1 μM of substrate per minute represents

the one unit of enzyme activity. All the enzyme assays were carried in duplicate and the total protein concentration was determined by Lowry's method using Bovine Serum Albumin (BSA) as the standard [19].

## 2.4. Analytics and calculations

### 2.4.1. Gas-chromatography–mass spectrometry

RO-16 and RB-5 degradation products were identified by a gas-chromatography–mass spectrometer (GC–MS). The GC/MS (GC–MS, Thermo Fisher Scientific Co., Ltd., USA) is equipped with a capillary column DB-5 (30 m × 0.25 mm). Helium was used as a carrier gas at a flow rate of 1 mL/min. The temperature-programmed mode in the GC column was as follows: initial temperature of the gasification compartment was set to 60°C held for 0.5 min, ramp at 235°C at a rate of 25°C/min, and held at this temperature for 2 min and then raised linearly to 250°C with a 2°C/min rate, held at this temperature for 5 min. Finally, the temperature was increased linearly to 280°C with a 15°C/min rate, and maintained for 5 min at this temperature. Sample volume and the retention time was 1 µL and 4 min, and the sample was injected without diversion. Scanning range of degraded products molecular weight was 45–600 m/z. Separated compounds were analyzed with the reference database NIST Mass Spectral Library search 2.0 mass spectral library [20].

### 2.4.2. UV-Vis and FTIR analysis

UV spectral analysis (190–900 nm) was done using UV-visible spectrophotometer (Lamda 35, Perkin Elmer, USA). The decolorization efficiency has been evaluated at  $\lambda_{\max}$  for RO-16 (490 nm) and RB-5 (597 nm). Samples were withdrawn aseptically at different intervals:

- OD at 600 nm of the sample mixtures without centrifugation:  
 $OD^{x+dye}$  at 600 nm =  $OD^{dye}$  +  $OD^x$ ;
- OD at 600 nm of sample supernatant after centrifugation for 10 min at 4,000 rpm:  
 $OD^{sup}$  at 600 nm =  $OD^{dye}$  at 600 nm; and
- OD of dye at  $\lambda_{\max}$  of sample supernatant after centrifugation:  
 $OD^{sup}$  at  $\lambda_{\max}$  =  $OD^{dye}$

The decolorization efficiency (DE) was determined as follows:

$$\%DE = \frac{(OD_i - OD_f)}{(OD_i)} \times 100 \quad (1)$$

Where  $OD_i$  and  $OD_f$  are the initial and final absorption of the dye at  $\lambda_{\max}$ . Fourier-transform infrared spectroscopy (FTIR) analysis was carried out using Perkin Elmer 783 Spectrophotometer and changes in percentage transmission at the mid IR region of 400–4,000  $\text{cm}^{-1}$  were recorded.

### 2.4.3. TOC and COD analysis

Total organic carbon (TOC) was determined using TOC analyzer (5050A, Shimadzu) by high temperature

catalytic oxidation method. TOC was calculated as follows:  $TOC = TC - TIC$ . Total carbon (TC) subtracted to the measured total inorganic carbon (TIC) where TC is the sum of organic carbon and inorganic carbon.

COD was recorded using a strong oxidant potassium dichromate method [21]. COD removal efficiency (%) during operation was estimated as follows:

$$\text{COD Removal}(\%) = \frac{\text{COD}(0) - \text{COD}(t)}{\text{COD}(0)} \times 100 \quad (2)$$

where COD (0) represents the initial COD (mg/L) or the COD at time  $t = 0$ , while COD ( $t$ ) represents the COD at any time  $t$ .

### 2.4.4. Power density

Potential (mV) measurements across the external resistance were recorded using a digital multimeter with a data acquisition system (Fluke 287 DMM). The current,  $I$  in milli-Amperes (mA) was calculated using Ohm's law:

$$I = \frac{V}{R} \quad (3)$$

where  $V$  is the measured voltage in millivolts (mV) and  $R$  is the external resistance in Ohms ( $\Omega$ ). The external load used in the experiment was 220  $\Omega$ . Power ( $\mu\text{W}$ ) was calculated using the formula  $P = IV$ , where,  $I$  and  $V$  represents current (mA) and voltage (mV), respectively. Power density ( $\mu\text{W m}^{-2}$ ) was measured by normalizing to the anode projected surface area ( $\text{m}^2$ ).

## 3. Results and discussions

### 3.1. Dye degradation in catholyte

Based on the presence of dye as catholyte or anolyte, various significant changes were observed on dye decolorization. Upon the addition of 0.5 mM of dye addition, only  $10.48\% \pm 0.5\%$  of dye decolorization (RO-16) was reported as cathode feeding. At a lesser concentration of 0.05 mM,  $45.27\% \pm 1.2\%$  of RO-16 decolorization was recorded, whereas the addition of dye in anolyte was resulted nearly complete decolorization (0.05 mM). Thus, effective removal was observed in anolyte compared to catholyte. Poorer performance of dye decolorization in cathode feeding might attributed to the non-biocatalytic activity and low electron transfer due to the absence of co-substrate (glucose) which is the rate determining factor for azo dye decolorization in MFCs [22]. Studies on five different catholytes were observed further to test the applicability of using the best catholytic solution on retrieving electrons via anode. Effective removal was observed using the following catholytes: Potassium permanganate, potassium ferricyanide, manganese dioxide, potassium chromate, and aromatic amines and the results were compared with phosphate buffer. Higher dye degradation was observed with phosphate buffer ( $86\% \pm 0.6\%$ ). For cells with potassium permanganate and potassium ferricyanide, the dye decolorization values tended to be  $69\% \pm 1.2\%$  and  $70\% \pm 1.2\%$  even after 9 d of inoculation. When potassium chromate was the catholyte, the dye degradation decreased to  $60\% \pm 0.8\%$  and manganese dioxide

remained with  $66\% \pm 0.9\%$  at its minimal. Similarly, for cells with aromatic amines as catholyte, the dye decolorization declined drastically during the initial 30 h, and reported only  $55\% \pm 1.7\%$  degradation (Fig. 1). The results clearly indicated the better the electrical activities in the cells with potassium permanganate and potassium ferricyanide due to elevation in the output voltage reduced the available electrons for dye reduction. Further, the results proved that manganese dioxide would also be a conductive electrolyte that influences more on electron transfer via anode rather than best electrolytic solution for dye degradation [23]. Bio-cathode with partially degraded dye containing aromatic amines was highly unstable due to higher proton accumulation which reduces the electrochemical activity and the degradation of dye also reduced [24]. Increasing the catholyte concentration of permanganate from 50 to 100 mM reduced the dye decolorization to  $50\% \pm 1.0\%$ , moreover, the pH of the catholyte at the end of MFC operation was also slightly higher ( $\text{pH } 8.0 \pm 0.3$ ) which could increase the overpotential and thus this would be a detrimental procedure to MFC performance.

### 3.2. Bioelectricity generation with different catholyte

Stable open-circuit voltage (OCV) was generated after 3 d of inoculation and MFC with dye feeding to the catholyte produced very less voltage than that obtained using PBS buffer. Potassium permanganate was accounted for a maximum OCV ( $1.15 \pm 0.05$  V) followed by potassium ferricyanide ( $0.56 \pm 0.01$  V); and manganese dioxide ( $0.52 \pm 0.02$  V); and potassium chromate ( $0.50 \pm 0.01$  V); and aromatic amines ( $0.46 \pm 0.01$  V); and phosphate buffer ( $0.43 \pm 0.01$  V) (Fig. 2). Voltage variation in potassium permanganate was found to be increased by two-fold compared to potassium ferricyanide. Thus, the potential gradient between the anode and cathode is higher due to improved electrical properties caused by potassium permanganate [25]. Availability of oxidizing agents as a terminal electron acceptor at cathode leads to the maximum reduction of electrons towards bioelectricity production [26]. Utilization of dye metabolites as a potential electron acceptor

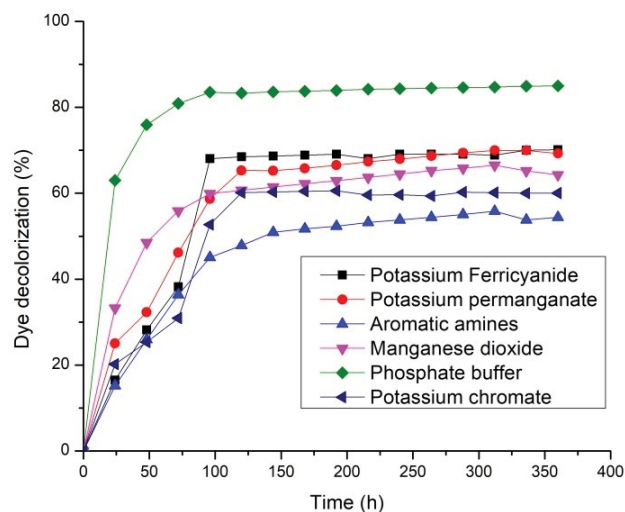


Fig. 1. Effect of different cathodic electron acceptor on dye decolorization.

in cathode because of the presence of the nitrogen group in place of oxygen was well correlated with lower azo dye degradation and considerable voltage generation but causes high voltage fluctuations. For cells using potassium permanganate, membrane fouling occurs over time that limited the protons transfer to the cathode even after post-treatment of the membrane with hydrogen peroxide [27].

### 3.3. Dye degradation in anolyte

MFC were supplied alternatively with different co-substrates such as glucose, glycerol, sucrose, acetate, and mannitol as studied previously [28]. Investigation on several types of anolyte with a different carbon source (carbohydrates and poly-alcohols) and comparative information of MFC performance on azo dye decolorization using micronutrients (synthetic wastewater) was represented in Fig. 3. The order of dye decolorization in descending was glucose ( $97\% \pm 0.8\%$ ) > sucrose ( $95\% \pm 0.5\%$ ) > acetate ( $83\% \pm 1.15\%$ ) > glycerol ( $60\% \pm 0.9\%$ ) > mannitol ( $15\% \pm 0.8\%$ ). Thus, the substrate glucose could be utilized effectively by the electroactive bacteria *P. aeruginosa* compared with other substrates. This condition detailed that decolorization was due to the bio-catalytic metabolism of microorganisms other than adsorption by cells. The decolorized intermediates of RO-16, mediated the electron transfer in MFC using pure strain of *P. aeruginosa*. Addition of decolorized liquid extraneously in anolyte decreases the RO-16 decolorization (49%). The addition of decolorized intermediates improved the OCV whereas in our case of RO-16 the addition of product intermediates has no effect on OCV [29]. The bacteria *P. aeruginosa*, have been demonstrated to contribute not only to the decolorization of azo dye but also to voltage output in the MFCs [30].

### 3.4. Bioelectricity production using different anolyte

In the experiments, the OCV was monitored for the different co-substrate (anolyte). For MSM medium without

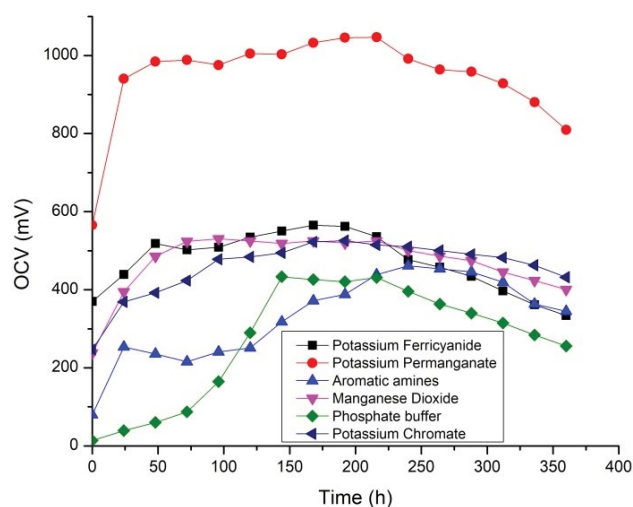


Fig. 2. Changes in open circuit potential during the treatment of RO-16 using different catholytes.

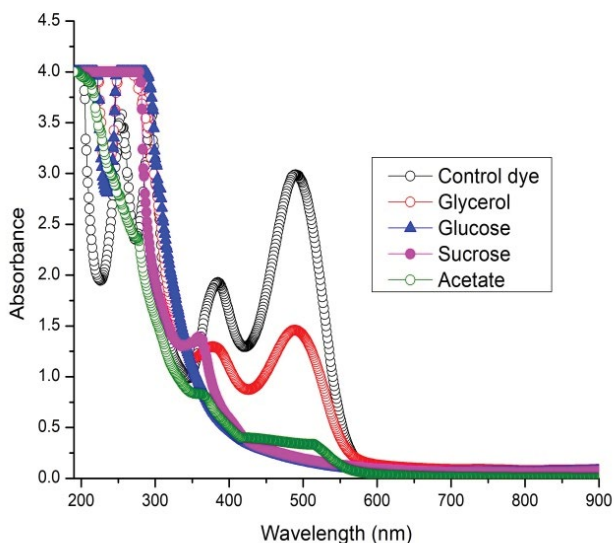


Fig. 3. UV-Vis spectra of RO-16 at different substrates on colour removal.

dye constituents, the potential of the anode decreased vastly from  $-10$  to  $-115$  mV. With glucose addition, the anode potential remains stable for 168 h ( $-290$  mV). With sucrose addition, the system stability increased to 240 h but the anode potential decreased to  $-327$  mV. Glycerol ( $-490$  mV) and acetate ( $-540$  mV) remains stable only for 48 h. Mannitol ( $-800$  mV) was highly unstable system and poor in terms of electrical performance and color removal (Fig. 4). The system stability of sucrose was higher compared with glucose because of the lower rate of degradation of sucrose. Glucose had increased the number of microorganisms in the anolyte from  $2 \times 10^6$  to  $12 \times 10^6$  CFU/mL, whereas the number of bacteria for sucrose was smaller ( $7 \times 10^6$  CFU/mL) than glucose. Thus, the growth of *P. aeruginosa* in glucose fed MSM (anolyte) would have produced more secondary metabolites (redox mediators) and improved the anode potential compared to other co-substrates [31]. Substrate affected differences in potential could attribute to the redox potential of the substrates used. Thus the potential difference between the substrates determines whether the redox process is favorable for electron recovery and transfer [27]. Reduction of azo dye would partially consume portions of electrons from the substrates and results in reduction in electron for electricity generation. Employing electricity generating bacteria is inevitable for the improved voltage recovery to overcome activity repression. Acclimated cultures of *P. aeruginosa* were tested for azo dye reduction with different co-substrates during 15 d of growth in anolyte. The culture condition yielded maximum power densities of  $1.9 \pm 0.18$  mW m $^{-2}$  (glucose),  $1.3 \pm 0.11$  mW m $^{-2}$  (sucrose),  $0.8 \pm 0.08$  mW m $^{-2}$  (glycerol),  $0.2 \pm 0.05$  mW m $^{-2}$  (acetate), and  $0.029 \pm 0.01$  mW m $^{-2}$  (mannitol). The bacterial metabolism was notably affected by the presence of glucose as co-substrate. Bacteria grown in mannitol fed MFCs showed very less electrochemical activity due to poorer growth in the adopted MSM medium. The same trend of growth was observed for co-substrates glucose, sucrose, and acetate (Fig. 5). The growth of *P. aeruginosa* in glucose fed MSM

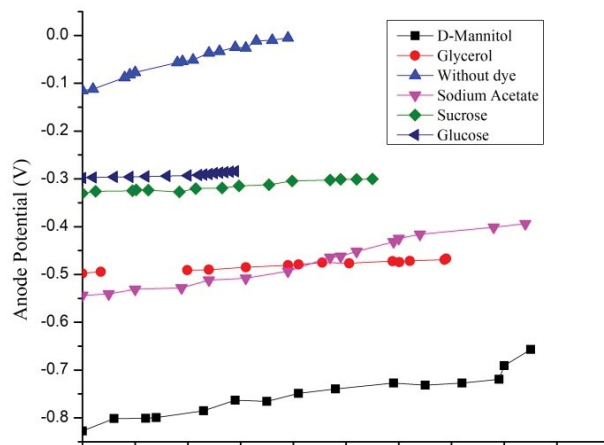


Fig. 4. Effect of anode potential by different substrates on power production.

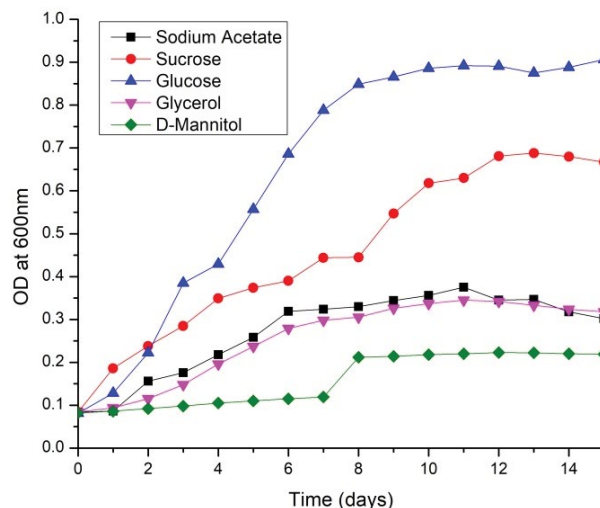


Fig. 5. Growth rate of *P. aeruginosa* on different substrates.

(anolyte) would have produced more secondary metabolites (redox mediators) and improved the anode potential compared to other co-substrates [31].

### 3.5. Effect of various dye concentrations

Effect of different concentrations of Reactive Orange 16 (mono-azo) and Reactive Black 5 (di-azo) was observed over 100, 200, 300, 500, 750, and 1,000  $\mu$ M. Dye decolorization was inhibited at 1,000  $\mu$ M for both the dye in the medium. Increasing concentration (1,000  $\mu$ M) of dye repressed the cell voltage, which caused a drastic decrease in cell OCV to  $181.02 \pm 1.6$  mV (RO-16) and  $84.26 \pm 0.9$  mV (RB-5) (Table 1). Consecutive cycles of redox potential (Fig. 6) were studied by the addition of dye from 100 to 500  $\mu$ M (RO-16) recorded similar results. Influent COD had increased with higher azo dye concentration with the same amount of glucose. Further the intermediates of dye after treatment could also contribute to a certain amount of COD in the MFC system.



Table 1  
Effect of various dye concentration on MFC performance

Model dye	Concentration ( $\mu\text{M}$ )	OCV <sub>max</sub> (mV)	Maximum COD removal (%)	Maximum decolorization (%)
RO-16	100	705	85	99
	200	692.3	70	98
	300	626.78	79	99
	500	500.01	77	85
	750	320.92	63	50
	1,000	180.35	50	24
RB-5	100	676	82	94
	200	640	78	92
	300	516.7	76	90
	500	428.75	75	74
	750	345.18	56	43
	1,000	85.54	42	10

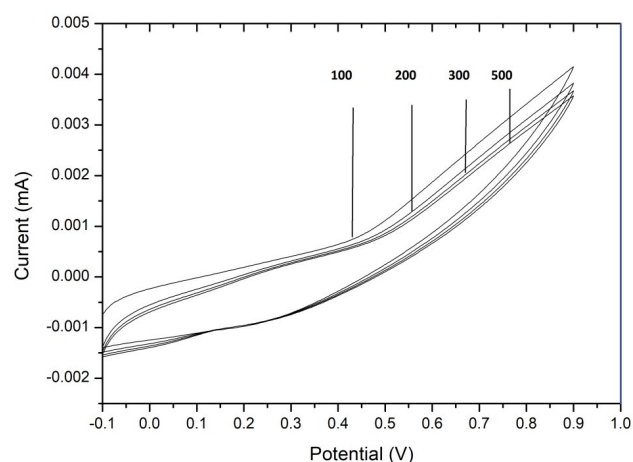


Fig. 6. CV response of different dye concentration (RO-16) on power output.

Increasing dye concentration leads to higher intermediates accumulation in the anode compartment which might have increased the COD thereby repressed the cell voltage. The proton and electron generated via microbial oxidation at the anode compartment were effectively used for monoazo dye degradation (RO-16) whereas the diazo dye (RB-5) required higher proton and electron generation from the substrate for its degradation. This could be the reason for higher degradability of RO-16 into simple intermediates as compared to RB-5. Effect of voltage generation on TOC and COD was investigated for RO-16 and RB-5. Fig. 7 indicates the oxidation of organic matter by MFC treatment. The carbon mass was investigated from the initial and residual TOC of the dye-containing solution at different treatment time. The degree of TOC removal was more than 95% for both the azo dye solution. Mineralization proceeded at faster rate for a high glucose concentration of 10 g/L with high consumption of electrical energy. It was observed that maximum COD removal of 85% for RO-16 and 82% for RB-5. Percentage COD reduction achieved in MFC is in close proximity to the reported values [32].

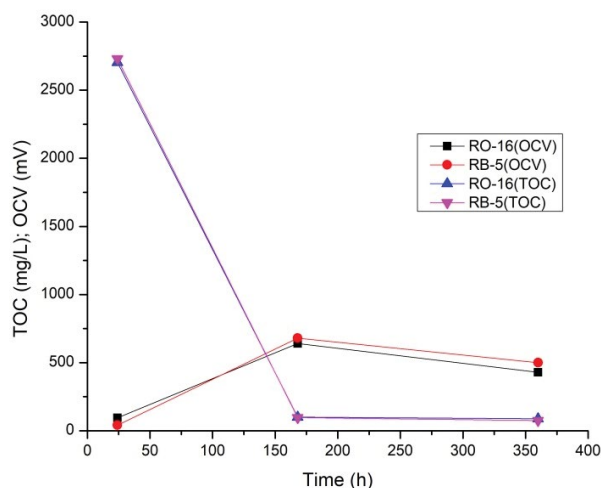


Fig. 7. TOC removal and energy production during the operation of MFC.

### 3.6. Analytical procedures

#### 3.6.1. Analysis of degradation

UV-VIS scan (190–900 nm) of supernatant were collected after 72 h and the major peak decreased in the region 490 nm (RO-16) and 597 nm (RB-5) and correspond to 99% and 94% of decolorization and disappeared completely. This evidence proved that the chromophoric group disappeared completely during the MFC process. FTIR spectral analysis of the untreated RO-16 and RB-5 after degradation in MFC results presented in Fig. 8 and the changes in percentage transmission were observed. Results of control showed peaks at 3,782; 3,343; 2,110  $\text{cm}^{-1}$ ; and 1,636  $\text{cm}^{-1}$  for  $-\text{NH}$  stretching, free  $-\text{NH}_2$  stretching,  $-\text{CH}_3$  stretching, and  $-\text{OH}$  stretching vibrations respectively. The peak at 1,081  $\text{cm}^{-1}$  for  $\text{S}=\text{O}$  indicates the presence of sulfoxide compound [33]. FTIR spectra of degradation product indicate peak at 3,311  $\text{cm}^{-1}$  for  $-\text{OH}$  stretching, a peak at 2,036  $\text{cm}^{-1}$  for  $\text{C}-\text{N}$  Stretching, supported by 1,636  $\text{cm}^{-1}$  for  $-\text{NH}$  stretching and a sharp peak at 601  $\text{cm}^{-1}$  indicates the degradation of aromatic amines. It was noticed

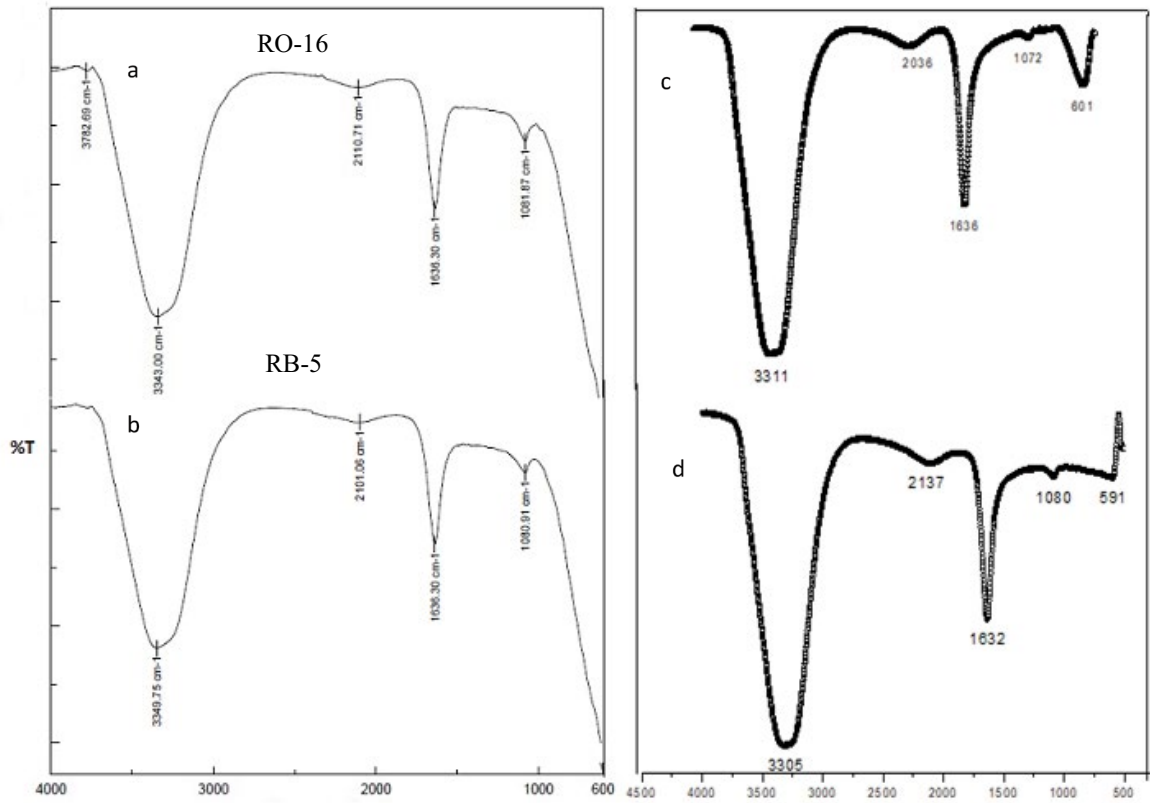


Fig. 8. FTIR spectra of RO-16 (monoazo) and RB-5 (diazo) before and after treatment.

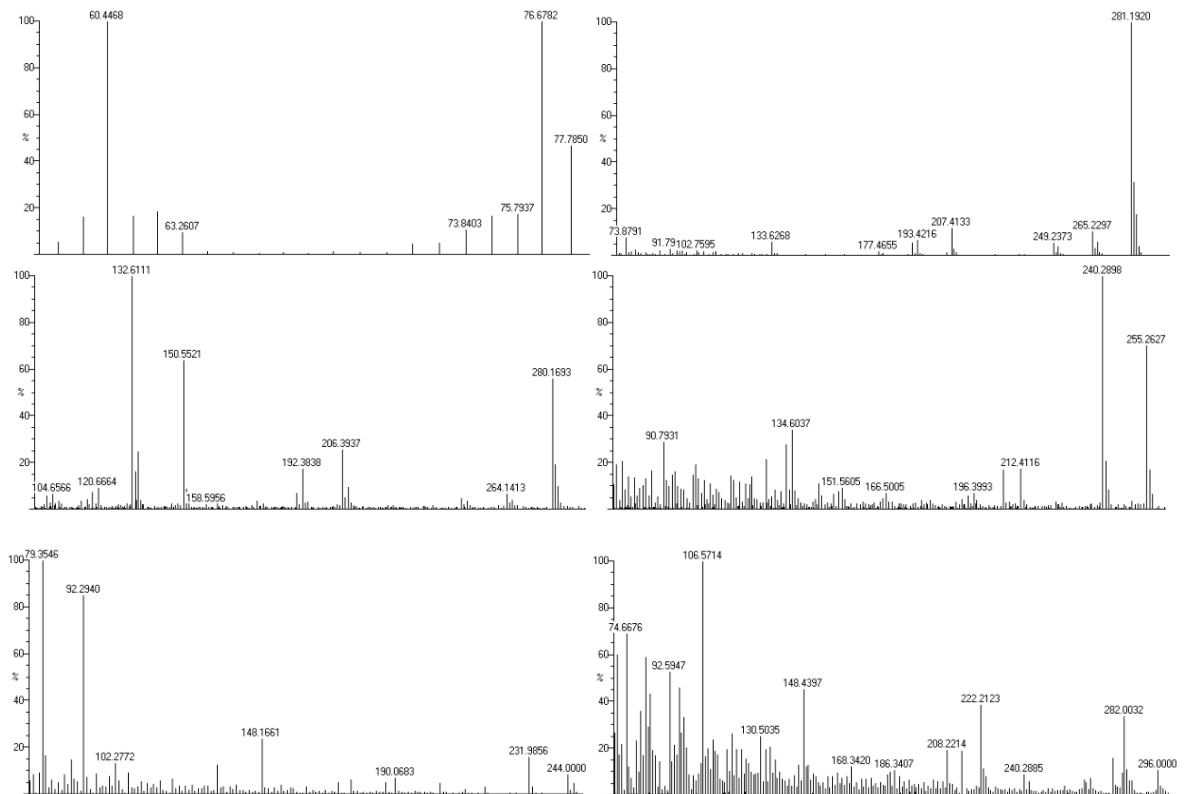


Fig. 9. Mass spectra of RO-16 intermediates after treatment.

that the  $\text{-NH}_2$  stretching vibrations were slightly shifted to lower energy region. FTIR spectral analysis of RB-5 showed a similar characteristic peak for control dye. The degradation product showed aliphatic C–N stretching and aromatic amine bending.

The GC–MS analysis revealed that MFC showed the breaking of the dye molecules into its metabolites. The Reactive Orange 16 was broken down into six metabolites (Fig. 9). Similarly, Reactive black 5 were broken down into five metabolites (Fig. 10). The dye degradation products confirmed that both the dye was degraded into simple molecules. 1,5-hexadiene from RO-16 is a hydrocarbon evident that the azo containing group degraded at the high extent in MFC system where the products are not harmful to the environment (Table 2). When comparing with the intermediates of RB-5, RO-16 had simple structures with lower molecular weight. If more time is given for the compounds in MFC, they would be further broken down (Table 3). Thus, MFC had proven to be a promising technology in terms of degradation of RO-16 and RB-5.

### 3.6.2. Elucidation with real textile effluent

Oxidation of real industrial effluent was studied and the results are shown in Fig. 11. In the UV-Vis spectra of

samples taken from real textile effluent, the fluorescent dye depicted maximum absorption at 266 nm, which diminished and resulted 78% of decolorization after treatment in MFC system. Hence, there was a possibility for the decolourising

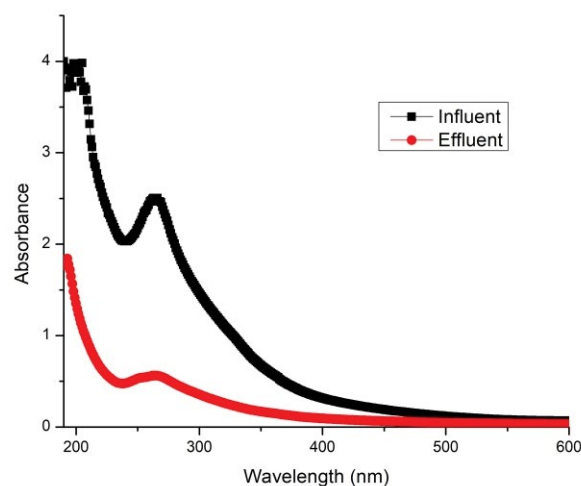


Fig. 11. Treatment of real industrial effluent in MFC using *P. aeruginosa*.

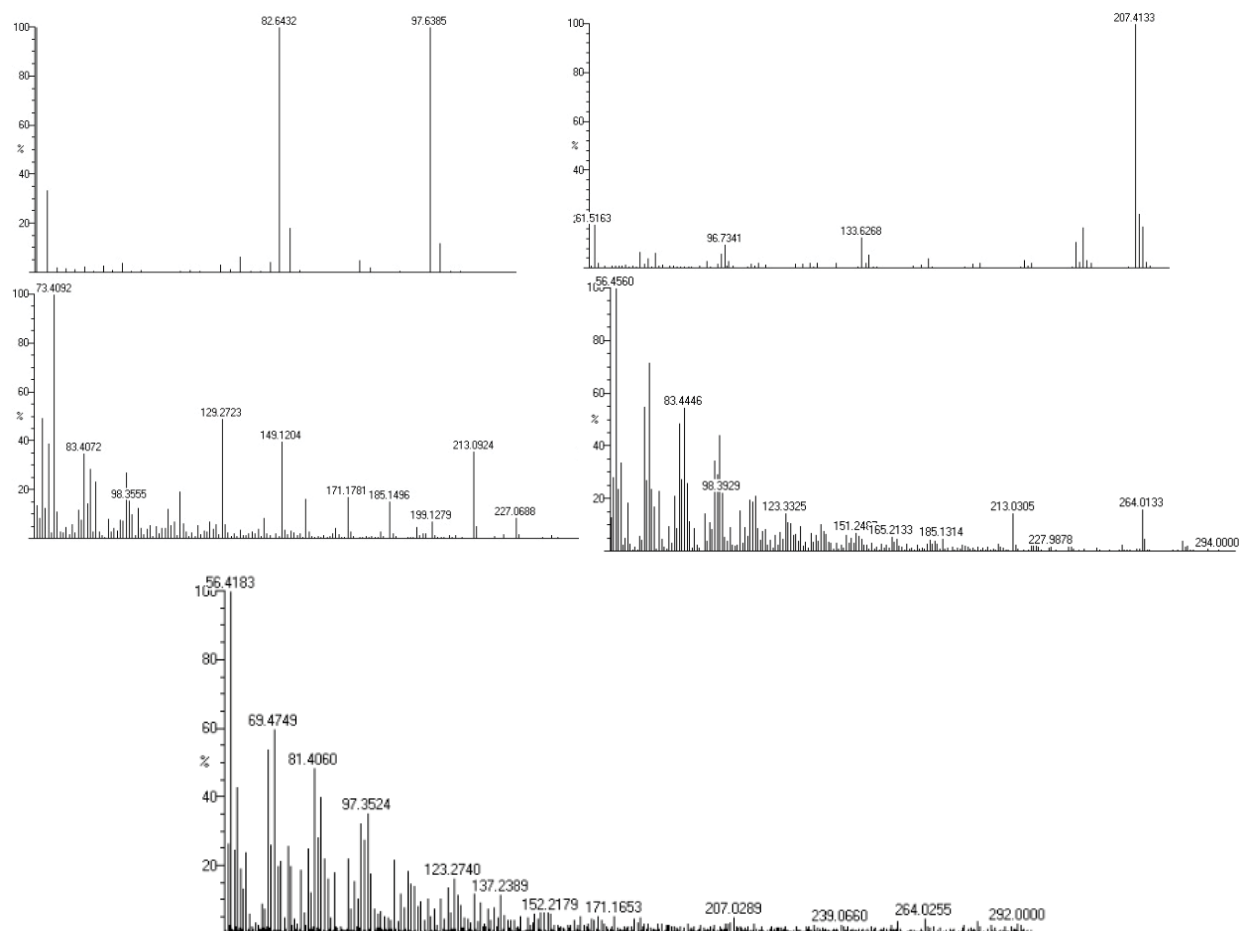


Fig. 10. Mass Spectra of RB-5 intermediates after treatment.



effect of the real dye wastewater. Further, the performance of MFC in terms of colour removal for real textile effluent was evaluated and the results are given in Table 4. MFC rapidly produced a stable voltage after inoculation, but the voltage output (614.5 mV) was relatively lower than potassium permanganate fed MFC. This finding indicated that the bacteria adapted well to the anodic environment containing real textile effluent.

### 3.7. Enzymatic analysis

Laccase and azoreductase activity were detected under anaerobic condition. A significant increase in the azoreductase activity was observed after degradation ( $1.54 \pm 0.01 \text{ U mg}^{-1} \text{ min}^{-1}$ ). Azoreductase activity was lower for diazo RB-5 ( $0.95 \pm 0.01 \text{ U mg}^{-1} \text{ min}^{-1}$ ) before the addition of dye but the laccase enzyme activity was not detected (Table 5). Decolorization of RO-16 and RB-5 within 48 h was 65% and 62%, respectively. The decolorization

Table 2  
GC-MS analysis results of the MFC effluent (RO-16)

Dye	Retention time (min)	MW	Degraded metabolites name
RO-16	3.27	78	1,5-hexadiene
	5.22	280	8H-pyrano[3,4-b]pyrimido[5,4-d]furane, 5,6-dihydro-4-hydrazino-6,6-dimethyl-2-methylthio
	9.62	280	3,4-dihydroisoquinoline, 1-[3-methoxybenzyl]-6-methoxy-
	11.37	255	1H-imidazo[4,5-c]pyridine, 2-[3,4-dimethoxyphenyl]-
	17	229	Phenol, 2,4-di[2-penten-4-yl]-6-methyl
	20.02	296	1-[1,2,3,4-tetrahydro-naphthalen-1yl]-3-p-tolyl-thiourea

Table 3  
GC-MS analysis results of the MFC effluent (RB-5)

Dye	Retention time (min)	MW	Degraded metabolites name
RB-5	3.97	83	2-amino-6-methylbenzoic acid
	6.93	206	Isoquinoline, 1,2,3,4-tetrahydro-6,7-dimethoxy-2-methyl-
	17.55	239	4,6-dimethyl-2-oxo-1-p-tolyl-1,2-dihydro-pyridine-3-carboxylic acid amide
	19.13	294	Benzenesulfonic acid, 4-nitro, 2-aminophenyl ester
	20.53	292	2-oxo-5-benzoxo-6-methyl-4-phenyl-1,2,3,4-tetrahydropyrimidine

Table 4  
Characteristics of real industrial effluent after MFC treatment

Parameter	Before treatment	After treatment
pH	7.2	7.8
COD	$1,380 \pm 30 \text{ mg/L}$	$980 \pm 30 \text{ mg/L}$
Total dissolved solids (TDS)	160 mg/L	88 mg/L
Total Suspended solids (TSS)	12 mg/L	10 mg/L
Conductivity	$3.25 \pm 1.0 \text{ mS/cm}$	$4.05 \pm 1.0 \text{ mS/cm}$

Table 5  
Enzyme activity in individual species in MFC

Enzyme	Dyes	Decolorization (%)	Enzyme activity before dye addition ( $\text{U mg}^{-1} \text{ min}^{-1}$ )	Enzyme activity after dye addition ( $\text{U mg}^{-1} \text{ min}^{-1}$ )
Laccase	RO-16	40	ND	$0.002 \pm 0.001$
Azoreductase	RO-16	65	$1.39 \pm 0.02$	$1.52 \pm 0.03$
Laccase	RB-5	38	ND	ND
Azoreductase	RB-5	62	$1.38 \pm 0.05$	$1.48 \pm 0.02$

ND, Not detected; Cells obtained for a period of 48 h; Values are the mean of maximum activity from two sets of experiments.

was due to the activity of azoreductase enzyme [17]. In the MFC chamber, the electrolyte was more electrophilic, and the larger portions of electrons were utilized for the azo bond cleavage.

#### 4. Conclusion

MFC treatment suggested that treatment of Reactive Orange 16 and Reactive Black 5 was most influential in anolyte with maximum power production. Degradation studies indicated that a reduction in reactive azo dye compound was most favorable. GC–MS analysis indicated the oxidation of aromatic amines improved the removal efficiency. Furthermore, azoreductase enzyme was found to be promising to reduce the azo bond.

#### Acknowledgment

We thank UGC, India for support with doctoral fellowship (to Ilamathi R – F1 – 17.1/2014-15/RGNF-2014-15-SC-TAM-58583).

#### References

- [1] L. He, P. Du, Y. Chen, H. Lu, X. Cheng, B. Chang, Z., Wang, Advances in microbial fuel cells for wastewater treatment, *Renewable Sustainable Energy Rev.*, 71 (2017) 388–403.
- [2] C.I. Pearce, J.R. Lloyd, J.T. Guthrie, The removal of colour from textile wastewater using whole bacterial cells: a review, *Dyes Pigm.*, 58 (2003) 179–196. doi: 10.1016/S0143-7208(03)00064-0.
- [3] L.S. Andrade, T.T. Tasso, D.L. da Silva, R.C. Rocha-Filho, N. Bocchi, S.R. Biaggio, On the performances of lead dioxide and boron-doped diamond electrodes in the anodic oxidation of simulated wastewater containing the Reactive Orange 16 dye, *Electrochim. Acta*, 54 (2009) 2024–2030.
- [4] B.E. Logan, J.M. Regan, Microbial fuel cells — challenges and applications, *Environ. Sci. Technol.*, 40 (2006) 5172–5180.
- [5] S. Kalathil, J. Lee, M.H. Cho, Granular activated carbon based microbial fuel cell for simultaneous decolorization of real dye wastewater and electricity generation, *New Biotechnol.*, 29 (2011) 32–37.
- [6] S.K. Chaudhuri, D.R. Lovley, Electricity generation by direct oxidation of glucose in mediatorless microbial fuel cells, *Nat. Biotechnol.*, 21 (2003) 1229–1232.
- [7] H. Liu, S. Cheng, B.E. Logan, Production of electricity from acetate or butyrate in a single chamber microbial fuel cell, *Environ. Sci. Technol.*, 39 (2005) 658–662.
- [8] J.R. Kim, S.H. Jung, J.M. Regan, Electricity generation and microbial community analysis of alcohol powered microbial fuel cells, *Bioresour. Technol.*, 98 (2007) 2568–2577.
- [9] R. Ilamathi, J. Jayapriya, Microbial fuel cells for dye decolorization, *Environ. Chem. Lett.*, 16 (2018) 239–250.
- [10] K. Rabaey, J. Keller, Microbial fuel cell cathodes: from bottleneck to prime opportunity?, *Water Sci. Technol.*, 57 (2008) 655–659.
- [11] H. Rismani-Yazdi, S.M. Carver, A.D. Christy, O.H. Tuovinen, Cathodic limitations in microbial fuel cells: an overview, *J. Power Sources*, 180 (2008) 683–694.
- [12] S.V. Mohan, G. Mohanakrishna, B.P. Reddy, R. Saravanan, P.N. Sarma, Bioelectricity generation from chemical wastewater treatment in mediatorless (anode) microbial fuel cell (MFC) using selectively enriched hydrogen producing mixed culture under acidophilic microenvironment, *Biochem. Eng. J.*, 39 (2008) 121–130.
- [13] S. You, Q. Zhao, J. Zhang, J. Jiang, S. Zhao, A microbial fuel cell using permanganate as the cathodic electron acceptor, *J. Power Sources*, 162 (2006) 1409–1415.
- [14] J. Sun, B. Cai, Y. Zhang, Y. Peng, K. Chang, X. Ning, G. Liu, K. Yao, Y. Wang, Z. Yang, J. Liu, Regulation of biocathode microbial fuel cell performance with respect to azo dye degradation and electricity generation via the selection of anodic inoculum, *Int. J. Hydrogen Energy*, 41 (2016) 5141–5150.
- [15] B.E. Logan, C. Murano, K. Scott, N.D. Gray, I.M. Head, Electricity generation from cysteine in a microbial fuel cell, *Water Res.*, 39 (2005) 942–952.
- [16] S. Pandit, A. Sengupta, S. Kale, D. Das, Performance of electron acceptors in catholyte of a two-chambered microbial fuel cell using anion exchange membrane, *Bioresour. Technol.*, 102 (2011) 2736–2744.
- [17] A.A. Kadam, A.A. Telke, S.S. Jagtap, S.P. Govindwar, Decolorization of adsorbed textile dyes by developed consortium of *Pseudomonas* sp. SUK1 and *Aspergillus ochraceus* NCIM-1146 under solid state fermentation, *J. Hazard. Mater.*, 189 (2011) 486–494.
- [18] J.P. Jadhav, D.C. Kalyani, A.A. Telke, S.S. Phugare, S.P. Govindwar, Evaluation of the efficacy of a bacterial consortium for the removal of color, reduction of heavy metals and toxicity from textile dye effluent, *Bioresour. Technol.*, 101 (2010) 165–173.
- [19] O.H. Lowry, N.J. Rosebrough, A.L. Farr, R.L. Randall, Protein measurement with the Folin phenol reagent, *J. Biol. Chem.*, 193 (1951) 265–275.
- [20] X. Cao, H. Wang, X. Li, Z. Fang, X. Li, Enhanced degradation of azo dye by a stacked microbial fuel cell-biofilm electrode reactor coupled system, *Bioresour. Technol.*, 227 (2017) 273–278.
- [21] Hach Company, *Water Analysis Handbook*, 2nd ed., Hach Company, Loveland, 1992.
- [22] M.Z. Khan, S. Singh, S. Sultana, T.R. Sreerishnan, S.Z. Ahammad, Studies on the biodegradation of two different azo dyes in bioelectrochemical systems, *New J. Chem.*, 39 (2015) 5597–5604.
- [23] Q. Wen, S. Wang, J. Yan, L. Cong, Z. Pan, Y. Ren, Z. Fan, MnO<sub>2</sub> graphene hybrid as an alternative cathodic catalyst to platinum in microbial fuel cells, *J. Power Sources*, 216 (2012) 187–191.
- [24] M. Li, M. Zhou, X. Tian, C. Tan, C.T. Mcdaniel, Microbial fuel cell (MFC) power performance improvement through enhanced microbial electrogenicity, *Biotechnol. Adv.*, 36 (2018) 1316–1327.
- [25] W. Chin-Tsan, Y. Che-Ming, C. Zih-Sheng, L. Yao-Cheng, Performance of straw-fed microbial fuel cells with mixed rumen microorganisms by using different catholytes, *Biomass Bioenergy*, 59 (2013) 412–417.
- [26] D.K. Yeruva, J.S. Sravan, S.K. Butti, J.A. Modestra, S.V. Mohan, Spatial variation of electrode position in bioelectrochemical treatment system: design consideration for azo dye remediation, *Bioresour. Technol.*, 256 (2018) 374–383.
- [27] Y. Li, S. Pichiah, S. Ibrahim, Facile reconstruction of microbial fuel cell (MFC) anode with enhanced exoelectrogens selection for intensified electricity generation, *Int. J. Hydrogen Energy*, 42 (2016) 1661–1671.
- [28] P. Pandey, V.N. Shinde, R.L. Deopurkar, S.P. Kale, S.A. Patil, D. Pant, Recent advances in the use of different substrates in microbial fuel cells toward wastewater treatment and simultaneous energy recovery, *Appl. Energy*, 168 (2016) 706–723.
- [29] B.Y. Chen, M.M. Zhang, Y. Ding, C.T. Chang, Feasibility study of simultaneous bioelectricity generation and dye decolorization using naturally occurring decolorizers, *J. Taiwan Inst. Chem. Eng.*, 41 (2010) 682–688.
- [30] K. Watanabe, Recent developments in microbial fuel cell technologies for sustainable bioenergy, *J. Biosci. Bioeng.*, 106 (2008) 528–536.
- [31] K. Rabaey, N. Boon, M. Hofte, W. Verstraete, Microbial phenazine production enhances electron transfer in biofuel cells, *Environ. Sci. Technol.*, 39 (2005) 3401–3408.
- [32] K.M. Kodam, I. Soojhawon, P.D. Lokhande, K.R. Gawai, Microbial decolorization of reactive azo dyes under aerobic conditions, *World J. Microbiol. Biotechnol.*, 21 (2005) 367–370.
- [33] D.C. Kalyani, P.S. Patil, J.P. Jadhav, S.P. Govindwar, Biodegradation of reactive textile dye Red BLI by an isolated bacterium *Pseudomonas* sp. SUK1, *Bioresour. Technol.*, 99 (2008) 4635–4641.